THE SHARCS PROJECT: SMART HYBRID ACTIVE ROTOR CONTROL SYSTEM FOR NOISE AND VIBRATION ATTENUATION OF HELICOPTER ROTOR BLADES

Fred Nitzsche and Daniel Feszty
Department of Mechanical and Aerospace Engineering
Carleton University
Ottawa, ON, K1S 5B6, Canada

David Waechter
Sensor Technology Ltd.
Collingwood, ON, L9Y 3Z4, Canada

Emanuele Bianchi
Agusta S.p.A.
Via G. Agusta, 520 – 21017 – Cascina Costa di Samarate (VA), Italy

Spyros Voutsinas
Aerodynamics Laboratory
National Technical University of Athens
Zografou Campus, 15773, Athens, Greece

Massimo Gennaretti
Department of Mechanical and Industrial Engineering
University Roma Tre
Via della Vasca Navale, 84 – 00146 – Rome, Italy

Giuliano Coppotelli
Department of Aerospace Engineering
University of Rome “La Sapienza”
Via Eudossiana, 18 – 00184 – Rome, Italy

Gian Luca Ghiringhelli
Department of Aerospace Engineering
"Politecnico di Milano" Technical University
Via La Masa, 34 – 20158 – Milan, Italy

ABSTRACT

The SHARCS project aims to develop an actively controlled helicopter rotor for the simultaneous suppression of vibration and noise. The proposed rotor will incorporate three subsystems of active control: an active impedance control device, which will replace the classical pitch link rods to reduce vibrations transmitted to the rotor hub, an actively controlled trailing edge flap to reduce vibrations due to dynamic stall and BVI as well as to reduce noise, and an actively controlled anhedral tip for the reduction of noise. The project is an international effort of seven partner institutions from Canada, Italy and Greece, which goal is to design, build and wind tunnel test a scaled rotor incorporating all three subsystems. The present paper describes the project structure and the progress made in the individual areas of research and design in the first year of the project.

Introduction

It is expected that the next generation of helicopters will incorporate active control devices to suppress noise and vibration. One of the most advanced active control techniques to attenuate noise and vibration in helicopters is called individual blade control (IBC), where each blade is individually commanded independently of its azimuth angle. In the past, IBC was not fully developed due to the lack of actuators able to withstand the loads that characterize the helicopter rotor environment. Among the new solutions to achieve efficient IBC, the ones that involve solid-state actuators – "smart" structures are seen as the most promising.

The SHARCS project is expected to demonstrate the ability of the smart structures systems, employing multiple active materials actuators, sensors and closed-loop controllers, to reduce both vibration and noise in rotorcraft. An articulated four bladed rotor model, Mach and aeroelastically scaled, will be tested in wind tunnel in 2007 at the Politecnico di Milano facility, using an Agusta S.p.A. test rig.

The project is co-sponsored in Canada by NSERC (Natural Sciences and Engineering Research Council) and the Ontario Centre of Excellence MMO (Materials Manufacturing of Ontario). The research also counts with the financial support of Sensor Technology Ltd., a company specialized in the production of smart sensors and actuators, which is based in Collingwood, Ontario, Canada and a major helicopter manufacturer, Agusta S.p.A. of Italy. Carleton University coordinates the entire project, providing the various designs of the active controls subsystems and it is also responsible for the development of the related software. Sensor Technology contributes by supplying the necessary smart actuators and by supporting the smart subsystems solutions with its engineering team. Agusta S.p.A. not only provides the noise and vibration suppression requirements of a typical helicopter rotor but, most importantly, it also supplies the scaled rotor hub mechanism, the scaled blade hardware, and the slip ring rotor data collection system. Other international partners responsible for specific tasks of the project include the "Politecnico di Milano" Technical University in Milan (POLIMI), University of Rome "La Sapienza", the Third University of Rome (Roma Tre) of Italy, and the National Technical University of Athens (NTUA) of Greece.

The SHARCS Project Concept

The most important components of noise and vibration produced in helicopters are originated in the main rotor from the unsteady aerodynamics that characterizes high-speed forward, manoeuvring and descent flight regimes. Low-frequency vibration is mostly generated by dynamic stall in the reverse-flow region at high forward speeds, whereas high-frequency acoustic noise is produced mainly in manoeuvring and descent flight regimes when the rotor blades interact with the vortices shed by the tip of preceding blades, resulting in the phenomenon known as Blade Vortex Interaction (BVI). This interaction leads to an impulsive change in the blade loading that generates a pressure perturbation in the flow field above and below the rotor disk. The perturbation that propagates as a sound wave below the rotor disk reaches the ground in the form of a strong slapping noise.

Recent experiments with IBC in Europe indicated that both noise and vibration could only be reduced marginally at the same time, although significant reductions of each individually were reported (Ref. 1). The explanation for this fact would be the apparent conflict of the philosophy used in the control objectives, i.e. "smoothing" the flight of the blade for the objective of vibration reduction and, at the same time, avoiding intersection with the path of the impinging vortices for the objective of noise attenuation.

The main aim of the SHARCS project is therefore to develop a "hybrid" control concept consisting of separate flow and structural control subsystems. An idealization of such an approach is seen in Fig. 1. This approach would have potential to reduce noise and vibration simultaneously, in part because the problems of vibration and noise are handled by two completely independent feedback subsystems. According to Fig. 1, the Smart Spring actuator (Ref. 2) placed at the blade root would attenuate the vibration whereas the active shape control at the tip of the blade would reduce the noise.

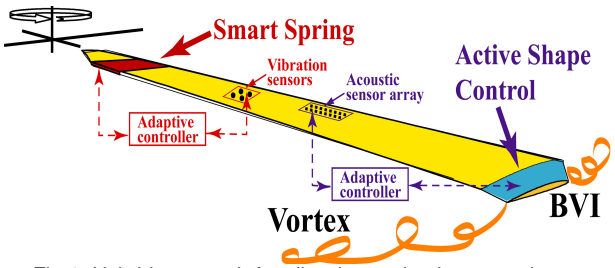

Fig.1: Hybrid approach for vibration and noise control on a helicopter rotor blade.

The Smart Spring is an active vibration control concept that uses piezoceramic actuators to preferentially vary dry friction and stiffness of a structure. This device, if located at the blade root, could adaptively vary the dynamic stiffness of the blade to change its flexural characteristics. It is this change of the flexural characteristics that allows the control of the aeroelastic response of the entire blade. A real-time controller identifies the variations in the structural dynamics due to the unsteady aerodynamic environment and maximizes the performance. Simulations and laboratory tests have already verified the ability of the Smart Spring to adaptively vary the structural impedance properties to suppress low-frequency torsional aeroelastic response of a fixed wing to buffet loads (Ref. 3).

As an addition to the Smart Spring, a suitably actuated trailing-edge flap would perform flow control by alleviating the negative effects of dynamic stall on the retreating blades, reducing the vibration excitation loads at their origin (Ref 4). In this reference, not only the size of the flap was shown to be relatively small, causing little conflict with the structural integrity of the blade, but also very little actuator loads were demonstrated. However, the latter is not seen as the only purpose of the addition of a flap. BVI causes large fluctuations in lift on the advancing side of the rotor disk. Since a flap can directly change the lift of an airfoil, it also has the potential to compensate for this undesired effect. When the lift suddenly increases due to the vortex passage, the flap can be deflected upward to reduce the overall lift and in the opposite sense when the lift is decreasing.

Finally, it has been demonstrated in separate studies that optimization of the blade anhedral tip angle can alleviate BVI at a fixed rotor attitude by displacing the trajectory of the vortices shed at the tip of the blade (Ref. 5). An adaptive mechanism taking advantage of this fact would be a flow control device specialized to perform noise control at flight conditions such as landing. As the blades travel through the air, each one of them sheds a helical tip vortex. In certain flight regimes, including landing, the blade can interact with the tip vortex of the preceding blades. The most critical type of such interaction is parallel BVI, in which the vortex axis is parallel to the leading edge of the blade. The superposition of the free stream velocity, rotor speed, and the velocity induced within the vortex leads to the high speed movement of the stagnation point around the leading edge, causing compressibility effects and emission of a loud, percussive noise.

There are two simple and obvious mechanisms to prevent this BVI noise effect. The first involves the increase of the so-called “miss distance” between the vortex centre and the blade. The second approach is to decrease the peak velocity in the vortex by increasing the vortex core diameter.. Increasing the vortex core diameter has the net effect of reducing the peak tangential velocity in the vortex, while not affecting the total vorticity within the vortex. This represents a paradigm in which variable tip anhedral can be extraordinarily useful. With the anhedral un-deflected, the aerodynamic design of the blade is unchanged from one optimized for steady level flight, and thus the most efficient in both rotor power to weight and fuel endurance. A deflection of the anhedral will move the tip location downwards, thus displacing the wake, and increasing miss distance. Further, the careful selection of design parameters can result in a variety of changes in the aerodynamics of the system, which can act to modify the distribution of the shedding of vorticity.

Feasibility Studies on the Hybrid Control Approach

Most of the current active vibration control research activities attempt to actively alter the time varying aerodynamic loads on the blade to suppress vibration. However, successful implementation of these approaches has been hindered by electromechanical limitations of smart material actuators, in particular that of small stroke. An impedance control device is designed to adaptively alter the stiffness, damping and effective mass of the blade to control the structural response. One example of such mechanism is shown in the conceptual drawing in Fig. 2, optimized to exploit the large stiffness and bandwidth of piezoelectric materials to perform an indirect-active vibration of axial loads.

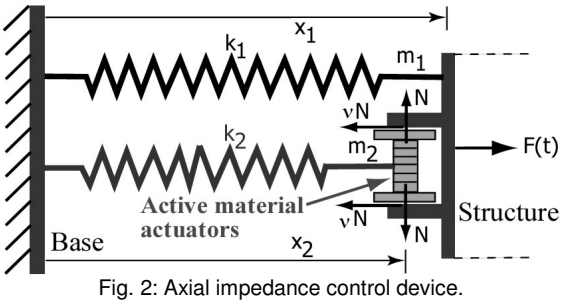

Fig. 2: Axial impedance control device.

The primary advantage of such system, compared to other piezoelectric actuator based approaches, is that the device does not rely on the piezoelectric actuators to achieve high stroke and force

simultaneously (meaning high power and high required voltages). Rather, the device only requires the actuators to produce micro displacements to generate relatively high actuation forces. As such, the stacked piezoelectric actuators are able to achieve sufficient forces with less than 100 V peak-to-peak. The feasibility of this type of system is thus enhanced due to the use of lower driving voltages.

Roma Tre has performed comparative studies to evaluate the behaviour of a "hybrid" system including a structural control subsystem comprised by the Smart Spring placed at the blade root and an axial impedance control device replacing the common pitch link. The flow control device consisted of a flap. The objective was to reduce the vibratory hub loads in forward flight configuration. In these studies, the smart spring was assumed to modify the bending dynamics of the blade and the axial impedance control device the torsional dynamics of the blade. A sketch of the blade with inclusion of all the control devices is shown in Fig. 3.

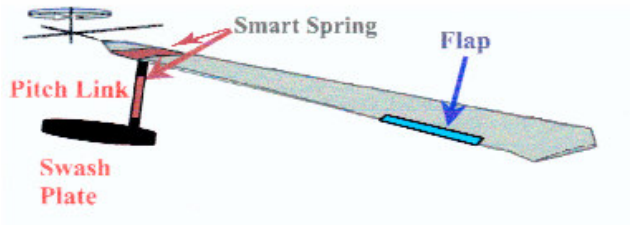

Fig. 3: Blade with Smart Spring, axial impedance control device and trailing edge flap studied by Roma Tre.

In the work carried out by Roma Tre, the basic-blade structural dynamics was described through the nonlinear flap-lag-torsion equations of motion presented by Hodges and Dowell (Ref. 6). These equations were related to a beam-like model, valid for straight, slender, homogeneous, isotropic, non-uniform, twisted blades. Retaining second order terms after the application of an ordering scheme that drops third-order terms not contributing to damping, and assuming radial displacements as simply geometric consequences of the transverse bending deflections the final form of the dynamic system is a set of coupled nonlinear integro-partial differential equations suitable for describing the response of helicopter rotor blades undergoing significant deflections.

$$\begin{aligned} m\ddot{v} + O_v\left[v, w, \phi, \dot{v}, \dot{w}, \theta, \dot{\theta}, \lambda_y, \lambda_z\right] &= L_v \\ m\ddot{w} + O_w\left[v, w, \phi, \dot{v}, \dot{w}, \theta, \dot{\theta}, \lambda_y, \lambda_z\right] &= L_w \\ J\ddot{\phi} + O_\phi\left[v, w, \phi, \dot{v}, k, \lambda_y, \lambda_z\right] &= M_\phi \end{aligned} \qquad (1)$$

The unknowns in (1) are the displacement of the elastic axis, *v(x,t)* and *w(x,t)* and the cross-section elastic torsion deflection, *Φ(x,t)*. In (1), O denotes a nonlinear operator, θ is the pitch angle distribution (given by superposition of twist and cyclic pitch), λ_y and λ_z denote respectively the blade flap and lead-lag bending stiffness, k denotes the torsion rigidity, m is the mass distribution, and J is the sectional moment of inertia. The forcing terms in the first two equations, L_v and L_w, are the generalized aerodynamic forces per unit length, whereas M_ϕ is the generalized aerodynamic moment also per unit length. In several rotor prediction tools that are commonly used by helicopter industries, the aeroelastic response of a helicopter rotor is analyzed by using two-dimensional, quasi-steady aerodynamic models with wake-inflow corrections (to take into account the 3D trailing vortices effect). These are based on the section loads given by either Theodorsen (Ref. 8) or Greenberg theory (Ref. 9) and under the assumption of very low-frequency analysis, for which the lift deficiency function is constant and equal to one. This restriction implies that the unsteady wake vorticity effects are neglected but introduces some simplification in the numerical analysis as it avoids computation of convolution integrals. In Roma Tre's work, a two-dimensional, quasi-steady aerodynamic model considering the wake inflow correction described by Drees (Ref. 10) was used to obtain L_v, L_w and M_ϕ.

For rotors in forward flight, the periodic aeroelastic response is obtained by applying the Galerkin method for the space discretization, followed by a harmonic balance approach for the time integration (Ref. 11). Vibratory hub loads are evaluated by combining the integration of inertial loads and aerodynamic loads along the span of each blade.

Structural Control Effect. Roma Tre investigated the possibility of reducing the vibratory hub loads through the action of cyclic-stiffness devices located both at the blade root and in the pitch link (applying the structural control devices only). The presence of the axial impedance control device in the pitch link required the introduction of an additional rigid-body rotation degree of freedom of the blade about the feathering axis, α. Thus, the angular position of an arbitrary blade section was given by the superposition of this degree of freedom with the elastic torsion (in addition to the rotation due to the cyclic pitch control):

$$\phi_{tot}(x,t) = \phi(x,t) + \alpha(t) \qquad (2)$$

The inclusion of the structural control devices does not alter the number of blade degrees of freedom. However, a time-dependent flap bending stiffness, λ_y^s, and lead-lag bending stiffness, λ_z^s, must be considered in the aeroelastic equations due to the presence of the Smart Spring (Ref. 12). Likewise, a time-dependent stiffness term, k_s must be included to take into account the axial impedance control device at the pitch link. The latter is related to the rigid-body rotation of the blade, and its effects were represented through a Dirac delta function located at the spanwise position of the pitch link. In fact, the presence of the rigid-body degree of freedom, in addition also influences all the aerodynamic forcing terms appearing in the aeroelastic equations (Ref. 12).

The core of Roma Tre's work was to identify the optimal cyclic variation of the stiffness, λ_y^s, λ_z^s and k_s for reducing the vibratory hub loads. This was achieved by minimizing the following cost function:

$$J = \tfrac{1}{2}\left((1-\eta)\mathbf{z}^T\mathbf{W}_z\mathbf{z} + \eta\mathbf{u}^T\mathbf{W}_u\mathbf{u}\right) \tag{3}$$

where **u** is the vector collecting the harmonics of λ_y^s, λ_z^s and k_s to be identified, **z** is the vector of the hub load harmonics to be reduced (at the frequency *N/rev* for a *N*-bladed rotor) and the superscript T designates the transpose. In addition, $\mathbf{W}_z$ and $\mathbf{W}_u$ are weight matrices defined so as to focus the minimization process on the critical variables, and η is a real number between 0 and 1 that measures the relative importance of the minimization of the control variables with respect to that of the vibratory loads. In order to determine the vector **u** that minimizes the functional J, the hub load harmonics were assumed related to **u** throughout a transformation matrix **T** as follows:

$$\mathbf{z} = \mathbf{z_0} + \mathbf{T}\mathbf{u} \tag{4}$$

where $\mathbf{z_0}$ denotes the baseline vibrating hub loads. The matrix **T** was obtained numerically (Ref. 12). Combining (1) and (3), the functional minimization yielded the optimal harmonics of , λ_y^s, λ_z^s and k_s:

$$\mathbf{u} = \left[(1-\eta)\mathbf{T}^T\mathbf{W}_z\mathbf{T} + \eta\mathbf{W}_u\right]^{-1}(1-\eta)\mathbf{T}^T\mathbf{W}_z\mathbf{z_0} \tag{5}$$

Rome Tre has applied this optimal approach for vibratory hub load reduction to the four-bladed BO-105 rotor having radius 4.93 m, constant chord 0.395 m, linear twist angle of –8 degrees, and with the structural parameters given in Ref. 13. It has examined in level flight conditions with rotational speed 40 rad/s at high advance ratios of 0.15 and 0.3.

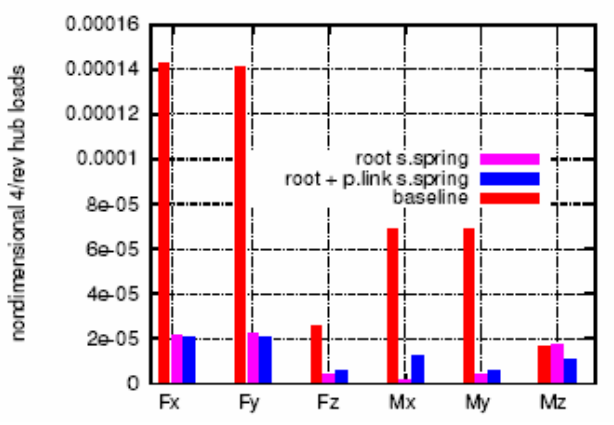

Fig. 4: Vibration levels for the blade including structural control devices studied by Roma Tre (advance ratio 0.15).

For the advance ratio 0.15, Fig. 4 depicts the comparison between the baseline vibratory hub loads to those obtained by activating the structural control devices. The figure shows that the devices allow an excellent reduction of the vibratory hub loads, even without the contribution of the axial one at the pitch link. However, the application of the axial impedance control device avoids the problem of an increase in the yawing moment that is typical to the use of controllable-stiffness devices (Ref. 14).

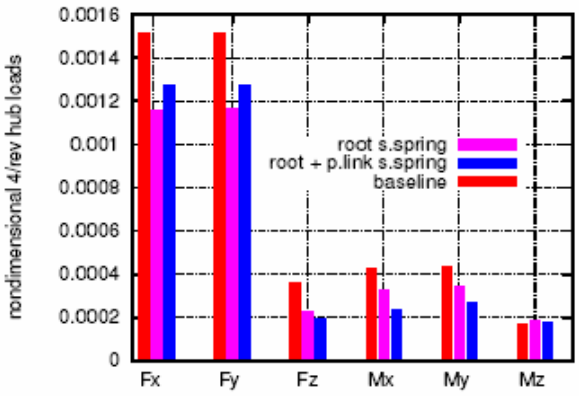

Fig. 5: Vibration levels for the blade including structural control devices studied by Roma Tre (advance ratio 0.30).

Fig. 5 presents the same comparison for the higher advance ratio 0.30. In this case, the reduction of the vibratory hub loads is lower than in the previous case; however the application of the axial controller at the pitch link is particularly useful in reducing the vertical force and the pitching and rolling moments (the yawing moment is prevented from increasing).

NTUA has also collaborated with Carleton University to develop computer simulations for the active rotor system using an adaptive structure, aeroelastic/

aeroacoustic research-oriented program that combines distinct aerodynamic, structural and aeroacoustic components in a time-domain solution where free-wake effects are included using a vortex-particle method. A complete description of the code capabilities can be found in a previous paper (Ref. 15). Independent studies confirmed that the insertion of the axial impedance control device at the pitch link was beneficial for the reduction of the axial transmitted loads. Fig. 6 indicates that the axial control device alone was able to filter the higher harmonics transmitted loads without affecting the lower harmonics associated to the blade pitch control. In this case, the control law was based on a maximum energy extraction principle (Ref. 16).

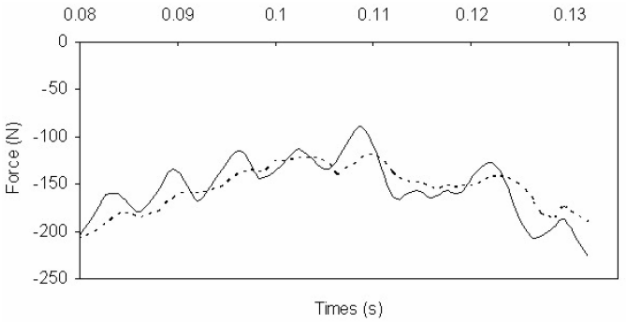

Fig. 6: Transmitted loads during one blade revolution for the baseline and structural control cases using the axial impedance control device (advance ratio 0.25). Study by Carleton University and NTUA.

Flow Control Effect. Roma Tre examined the reduction of the vibratory hub loads through the cyclic motion of a trailing edge flap. The presence of the flap modifies the governing equations given by Hodges and Dowell due to both of the introduction of additional inertial terms and its significant influence on the aerodynamic loads (Ref. 17). In the latter case, the aerodynamic loads were modified in agreement with the Theodorsen theory under the assumption of the quasi-steady approximation. Akin to the problem discussed previously, **u** collected the harmonics of the flap deflection. Minimization of a cost function shown in (3) yielded the optimal cyclic flap motion though the expression in (5). Several techniques may be applied for the evaluation of the transfer matrix **T**. For the present application, it was determined through an analytical procedure that allows a computationally very efficient search of the optimal control strategy.

The cyclic flap was applied to the same rotor examined in the previous section. The results corresponding to advance ratios 0.15 and 0.30 are shown in Figs. 7 and 8, respectively.

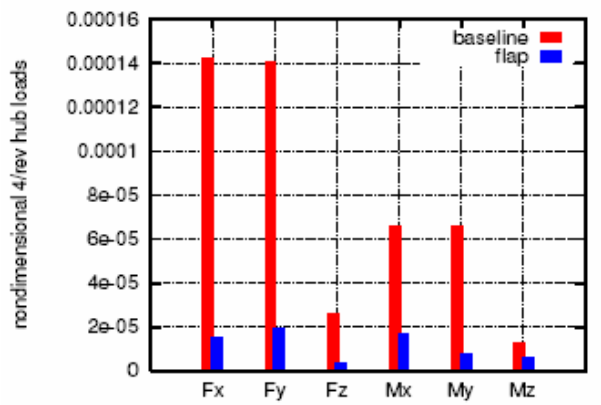

Fig. 7: Vibration levels for the blade with the flow control device (flap) studied by Roma Tre (advance ratio 0.15).

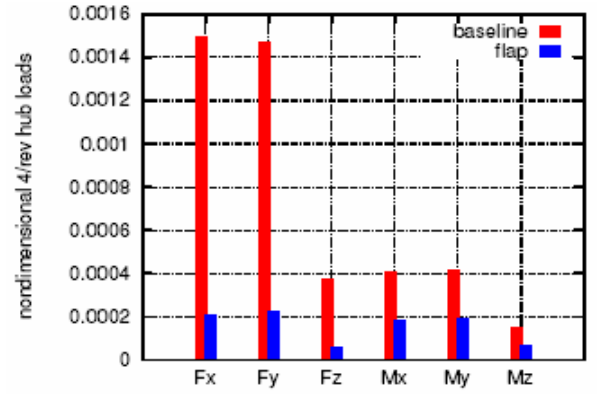

Fig. 8: Vibration levels for the blade with the flow control device (flap) studied by Roma Tre (advance ratio 0.30).

The comparison between the baseline vibratory hub loads and those arising during activation of the flap demonstrated that the cyclic flap motion is a very efficient way to reduce vibrations. However, when compared to what was observed with the application of the structural control devices, it indicated less robustness. Parametric studies suggested that a configuration having some differences with respect to that used for the control identification showed a significantly reduced efficiency. Finally, it is worth noting that both in the application of the structural and flow control devices the optimal harmonics of the controls identified were well within their limits of applicability.

CFD simulations of the Actively Controlled Flap

Vibrations on helicopter rotors arise due to inertial forces, structural loads and aerodynamic phenomena such as dynamic stall or BVI (Ref: Johnson). In the work performed at the Carleton University, the feasibility of the Actively Controlled Flap (ACF) for reducing vibrations due to dynamic stall were demonstrated via CFD.

Dynamic stall occurs at moderate to high advance ratios on the retreating blades and manifests itself in increased dynamic lift and nose-down pitching moments. These have the consequence of high vibratory loads transferred to the pitch links, which not only negatively affect the controllability of the rotorcraft but also set the limit for the maximum forward flight velocity of a helicopter. Hence, the aim of employing an ACF is logically to avoid dynamic stall or, for the flight regimes when this cannot be achieved, to mitigate its effects. Two actuation strategies will be considered.

For moderate advance ratios (μ = 0.25~0.30), when the retreating blades encounter light stall, it is proposed to deflect the flap downward. The increased lift coefficient due to the flap should allow for the same blade lift generated without entering dynamic stall. Hence, this strategy promises to reduce vibrations by delaying dynamic stall.

For high advance ratios, close to the helicopter's maximum forward flight speed, dynamic stall will be entered even if the flap is deflected downward. For this case, it is proposed to deflect the flap upwards so that the negative effects of dynamic stall can be mitigated.

Low advance ratio - downward flap deflection case

A 3D vortex particle method, GAST, developed at the National Technical University of Athens, was employed for the simulations (Ref. 18). This employs a grid-free discrete vortex formulation and as such is ideal for complex, moving multi-body problems, such as full 3D rotorcraft simulations. The code employs the ONERA model to account for the effects of dynamic stall. A four-bladed configuration of the SHARCS rotor was modeled with an embedded 15% chord trailing edge flap. The flap spanned from 0.7R to 0.9R of the rotor radius, i.e. the region most affected by dynamic stall. Forward flight corresponding to the advance ratio of μ = 0.30 was simulated. 105 revolutions were performed to achieve trimmed flight conditions. The results shown correspond to the last two revolutions.

The angle of attack history of the 0.75R blade section was used to verify that dynamic stall occurred in the uncontrolled (i.e. no flap actuation) case. Then, the flap was actuated downward according to the flap deflection history shown in Fig. 9. Note that the maximum flap deflection was 10 degrees downward, the actuation started in the 3rd quarter of the azimuth and lasted for about 1/3rd of the time period of revolution. The simulation was re-started from the uncontrolled solution so trimmed flight condition was achieved only after 23 revolutions this time.

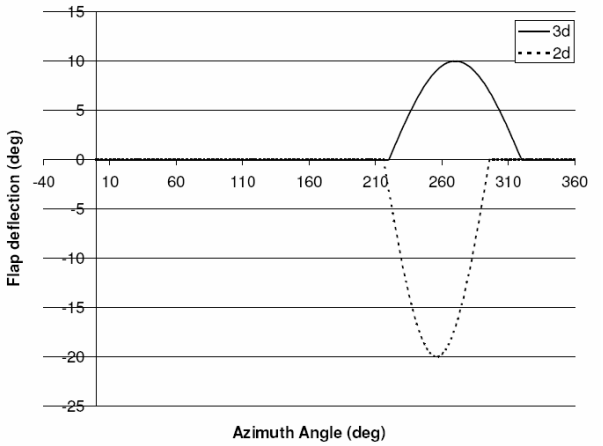

Fig. 9: Flap deflection histories for the 3D (solid line) and 2D (dashed line) simulations performed by Carleton University.

Comparison of the integrated blade root vertical loads and blade pitching moments for the uncontrolled and controlled cases are shown in Figs. 11 and 12, respectively. The blade pitching moment is representative of the pitch link loads since these transfer them to the control system.

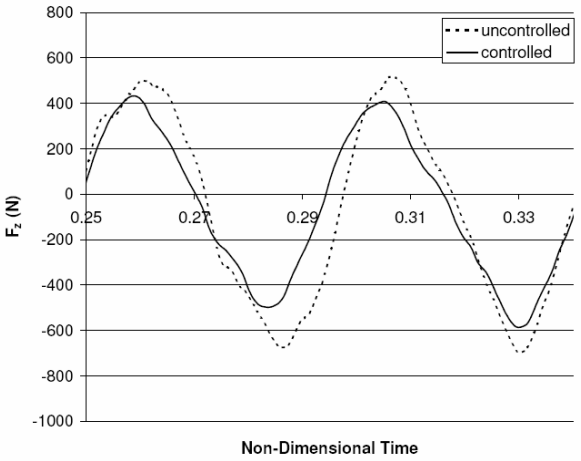

Fig. 11: Integrated blade root vertical loads from the 3D simulations. Study by Carleton University and NTUA.

As can be seen, the amplitude of the vertical hub shear loads was reduced in average by about 23% by actuating the flap. The reduction of the peak blade root torsional moments (and hence of the pitch link loads) is even more dramatic, about 44%. These results are very promising and suggest that dynamic stall induced vibrations can be significantly reduced by the ACF concept at moderate advance ratios.

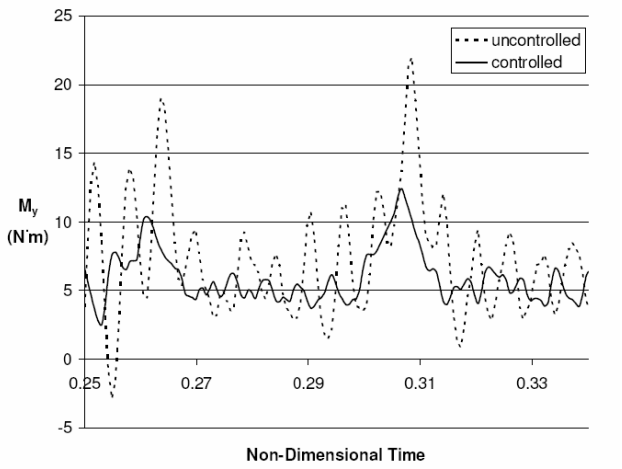

Fig. 12: Integrated blade root torsional moments from the 3D simulations. Study by Carleton University and NTUA.

High advance ratios - Upward flap deflection case

Since the ONERA dynamic stall model of the GAST code can only model the effects of dynamic stall but not to simulate them, it was necessary to use another CFD method to investigate the feasibility of the ACF concept for mitigating the effects of dynamic stall.

The CMB (Carleton Multi-Block) Navier-Stokes solver was used for the simulations. This is a structured, multi-block code based on the PMB code developed at the University of Glasgow (Ref. 19) and further modified in a number of areas, including enabling the actively controlled flap configurations. 2D simulations of a NACA 0012 airfoil in oscillatory motion were performed. The reduced frequency of motion was k=0.175, the mean angle of attack 15 degrees and the oscillation amplitude 10 degrees. Such case would be representative of a rotor blade section at 0.75R radius in high forward flight speed configuration. Parametric study of the effect of the flap size showed that a 20% chord flap yields the best result. Note that the flap deflection this time was 20 degrees up as shown by the dashed line in Fig. 9.

The general aim here was to reduce negative aerodynamic damping and stall flutter, which are characterized by the clockwise loops in the c_m-α curve (Ref. 4). The area of this loop is directly proportional to negative aerodynamic damping, so the aim was to reduce its size. Stall flutter has a major contribution to high levels of vibrations in the pitch link loads and essentially limits the maximum forward flight velocity attainable with a helicopter.
The comparison of the c_l-α and c_m-α loops for the uncontrolled and controlled cases is shown in Figs. 13 and 14, respectively.

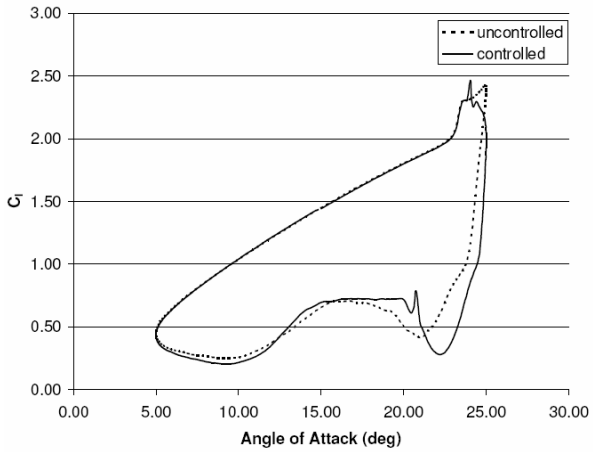

Fig. 13: c_l-α history for the NACA 0012 airfoil of the 2D simulations. Study by Carleton University.

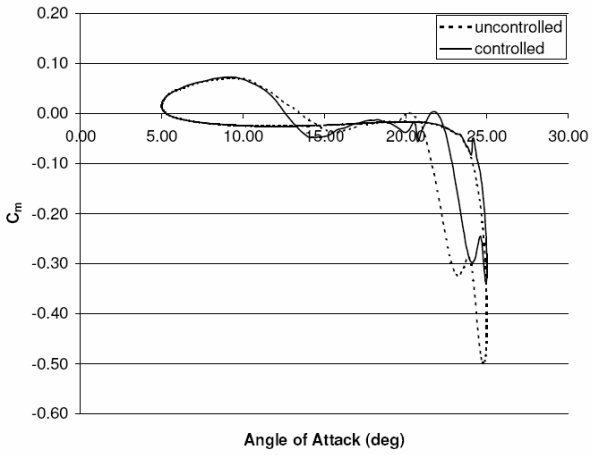

Fig. 14: c_m-α history for the NACA 0012 airfoil of the 2D simulations. Study by Carleton University

As can be seen, the second (clockwise) loop of the c_m-α curve has been significantly reduced by actuating the flap. The area of this loop and hence the value of negative aerodynamic damping was reduced by as much as 54%. Also note that at the same time, the penalty in dynamic lift is virtually negligible. The magnitude of the pitching moment coefficient has also been reduced by about 30%, implying lower pitch link loads.

These results indicate that even for the cases when dynamic stall cannot be avoided, the ACF concept with upward deflections can be successful in mitigating the negative effects of dynamic stall. Full details of the above simulations and analysis is presented in Ref. 20.

SHARCS Subsystems Hardware

In the current phase of the SHARCS project, three

actuators will be used to accomplish the "hybrid" control concept: (1) a new axial impedance control device will replace the rotor blade pitch link mainly to suppress the components of vibration loads originated by the excitation of the first torsional elastic mode of the blade, whose frequency is located near the critical frequency of 4/rev for a four bladed helicopter rotor. Importantly, the adaptability of the impedance control device will enable suppression of the aeroelastic response under a broader band of frequencies by altering the effective boundary conditions of the articulated blade and, consequently, the nature of the elastic modes of the rotating structure. The active vibration control system based on adaptive impedance control at the pitch link will be novel to the industry and it is seen as an effective approach to provide significant reduction in helicopter vibration. (2) A quasi-static shape control will adjust the anhedral angle at the tip of the blade to enable flow control and the optimization of noise level in descending flight regimes. (3) A flap at the trailing edge of the blade will be used with the dual purpose of structural and flow control depending on the flight regime. Each one of these actuators constitutes a subsystem of SHARCS along with the aeroelastically and Mach-scaled blade.

Subsystem Blade. The design of the typical section of a Mach scaled, aeroelastically similar composite rotor blade for wind tunnel testing is a responsibility of Carleton University. The ultimate purpose for designing this blade is to test a vibration and noise reduction system for helicopter blades. To be effective for this task, the blade must have the required vibration characteristics. Agusta provided the requirements for the SHARCS rotor as follows:

- Span = 1 m
- Composite construction
- Fully articulated
- Match the following rotating elastic natural frequencies:
  - 1^{st} flapping = 2.5 – 2.8/rev
  - 2^{nd} flapping = 4.2 – 4.7/rev
  - 1^{st} lead-lag = 4.5 – 5.5/rev
  - 1^{st} torsion = 5.5 – 6/rev
- Lock number = 5 – 6
- Tip speed = 0.6 Mach
- Centre of mass ≈ ¼ chord
- Number of blades = 4
- Hub radius = 0.126 m

The rotor blade was designed using a modified version of the DLR (German Aerospace Establishment) finite element program that was specifically prepared for building a scaled BO105 blade from composite material (Ref. 21). In this program, the properties of carbon fibre and glass fibre composites at different ply angles (0^o, 45^o, 90^o, etc.) are the input data. Having the composite properties, the program allows the operator to choose the type of composite and the number of plies at any station along with the profile of the rotor blade. Subsequently, the program calculates the bending and torsional local rigidities (EI, GJ), mass per unit length, centre of gravity, and the safety factor for the rotor blade. The purpose of using this program was to match GJ and EI with their corresponding target values roughly obtained using the isotropic beam approximation to find the eigenvalues of the rotating system. After several iterations, both the GJ and EI values converged to the target. The safety factor was also calculated at this stage of the process. The design was considered satisfactory when this safety factor was greater than 1.5. Two different criteria were used for determining the safety factor. One was based on the amount of stress and strength of the fibre, while the other was based on the amount of force required for the matrix to fail. To maintain a conservative design, the lowest of the two safety factor values was used at that location.

Table 1: Material Properties

Property	S-glass epoxy	IM6 epoxy
Fibre Volume Ratio	**0.5**	**0.66**
Density [g/cm^3]	**2.00**	**1.60**
E_1 [GPa]	**43**	**203**
E_2 [GPa]	**8.9**	**11.2**
G_{12} [GPa]	**4.5**	**8.4**
ν_{12}	**0.27**	**0.32**
Longitudinal tensile strength – [MPa]	**1280**	**3500**
Transverse tensile strength – [MPa]	**49**	**56**
Longitudinal compressive strength – [MPa]	**690**	**1540**
Transverse compressive strength –[MPa]	**158**	**150**
In-plane shear strength – [MPa]	**69**	**98**

The composites chosen were IM6/epoxy carbon fibre and S-glass/epoxy fibreglass with properties given in Table 1. Fibreglass was used for the 0^o plies, as any carbon fibre composites would result in a structure too stiff. It means that for the blade to have the target EI values only one ply of the carbon fibre would be necessary. Using one ply would result

in high stress that would exceed the tensile strength of the carbon fibre composite. Hence, a fibreglass construction was selected. As fibreglass is less stiff, more plies could be used to provide more structural thickness and reduce the axial stress due to the centrifugal loading. Even though fibreglass is heavier, the majority of the plies would be ahead of the ¼ chord, thereby reducing the amount of lead ballast required for the rotor blade to achieve the correct mass distribution properties. Thus, with the chosen design, a larger fraction of the mass of the blade becomes structural; hence increasing the structural efficiency. IM6 carbon fibre was used for the $\pm 45^{o}$ ply, as the off-axis stresses were orders of magnitude smaller than that produced by the axial centrifugal force. It means that only one ply could be used to provide acceptable safety factor and GJ values, with the added advantage of having less weight. Therefore, in this case, using a lighter composite design that requires less plies and yields less ballast reduced the total mass.

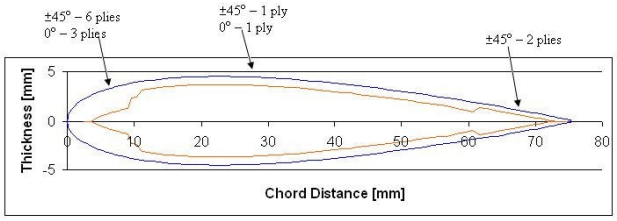

Fig. 15: SHARCS blade cross-section preliminary design.

The preliminary design of the cross section can be seen in Fig. 15. In order to keep the mass centre near the quarter chord position, more composite layers were placed at the nose than at the trailing edge of the airfoil. This creates a C-shaped nose spar, which carries most of the load. Even with the extra plies supplied by the fibreglass construction, 225 g of nose lead was required to shift the centre of gravity to the required 0.26 chord position. As a result, the total mass of the blade design without actuators was 489 g, which includes the 225 g of nose ballast. For this design, a minimum safety factor of 2.9 was obtained at the root of the blade, where the maximum resultant centrifugal force acts. The nose ply layup of $[0/45/-45/45/-45/45/-45/0/-45/45/-45/45/-45/45/0]_T$ degrees was used (where the subscript T means the total layup). It provided a balanced and symmetric laminate, which eliminates the coupling matrix, and ensures that there are no adjacent layers with identical angles. The general rule of thumb that there should not be more than three layers of the same orientation layered next to each other, as the layers will split (a generalized form of delamination) was imposed in the design. The symmetric layup was also maintained for the trailing edge of the rotor blade, while for the middle of the blade the anti-symmetric layup was kept because the anti-symmetric layup would induce no shear deformation due to the axial loading. It should be noted that "smoothing" of the ply edges shown in Fig. 15 should be considered in the manufacturing process to decrease the stress concentration in the sharp edges. Furthermore, a foam core was used in the centre of the rotor blade to prevent the skin from buckling or wrinkling. The foam core also transmits the shear to the composite lay up.

This design resulted in the stiffness values shown in Table 2. It proved exceedingly difficult to design a blade for which all three rigidities were in the correct range imposed by the SHARCS requirements. Still, although no 90^{o} plies were used, the lead-lag stiffness was 22% higher than the target value.

Table 2: Design versus Target Stiffness Values

	Design	Target	Difference [%]
EI_{xx} [Nm^2]	39.2	40	2.00
EI_{YY} [Nm^2]	1957	1600	22.31
GJ [Nm^2]	54.6	50	9.20

The preliminary design was verified by an analysis performed using the commercial package ANSYS. The fan plot for the articulated blade is shown in Fig. 16.

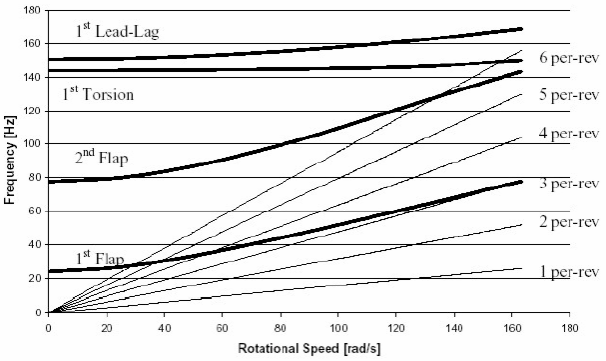

Fig. 16: SHARCS blade preliminary design fan plot.

The differences in the rotating frequencies between the preliminary blade design and the target values are shown in Table 3 at the nominal rotating frequency of 163 rad/s.

Table 3: SHARCS Blade Results

Composite Rotor Blade Rotating Natural Frequencies			
Articulated [per rev]	SHARCS at 163 rad/s	Design Requirement	Differenc [%]
1st Flap	3	2.5 - 2.8	7.14
2nd Flap	5.52	4.2 - 4.7	17.45
1st Lead-Lag	6.51	4.5 - 5.5	18.36
1st Torsion	5.79	5.5 - 6	0.00

Subsystem Structural Control. The structural control in SHARCS will be performed by an axial impedance control substituting the conventional pitch link, which is being entirely designed at Carleton University. The prototype system, which emulates the concept shown in Fig. 2, is presently under development (Fig. 17).

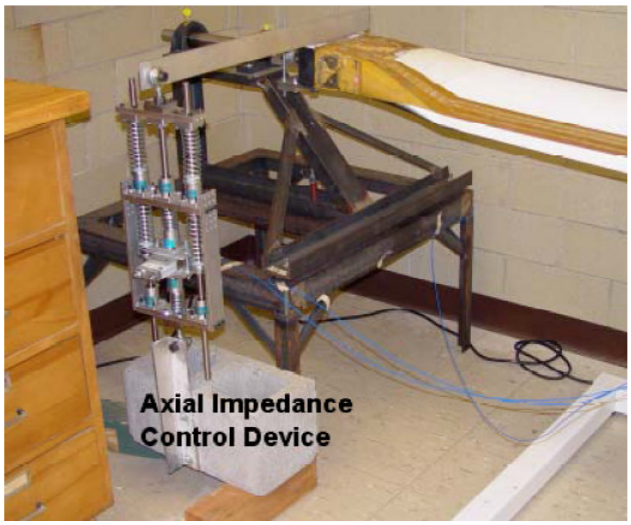

Fig. 17: SHARCS structural control device.

University of Rome "La Sapienza" is closely collaborating with Carleton University on the experimental system identification of the helicopter blade with the axial impedance control device. This is the first step of the general task of developing the structural control subsystem (software and hardware).

The effectiveness of the structural control subsystem will be tested during the experimental investigation considering first a non-rotating full-scale helicopter blade, and then the model Mach-scaled rotating blade. During the first experimental investigation concluded in August 2005, the whole procedure, aimed at identifying the modal parameter and dynamic response, was validated: a sensitivity of both natural frequencies and damping ratios to the different values of the adaptive impedance added to the pitch link was outlined. The effect on the blade dynamic responses, as a consequence of the different regimes of the adaptive impedance, was analyzed for the different levels of actuation. This experimental investigation provided useful information for further experimental activity related to the Mach-scaled rotating blade, in which the actual capability of the concept to reduce the vibration levels will be considered. In this activity, the development of a procedure capable to estimate the modal parameters from the measurements of only the responses of the structure will also be investigated and compared with the one achieved with the traditional experimental modal analysis (i.e. SIMO experimental analysis) using the LMS system identification software. The proposed approach has been already applied to a wide range of structures giving reliable results in several modal analysis tasks, such as model updating, vibration level estimation, fatigue analysis, where the actual loading and operating conditions are important for the structural response, (Refs. 22, 23). The main hypothesis of this so called "Output-Only" analysis, rely on the type of the excitation loading that is considered as a white noise (both in time and in space) at least in the frequency band of interest. The advantages of identifying modal parameters from the ambient excitation and then considering the system with the actual operational conditions will make this approach of paramount interest, (Refs. 24, 25), especially when dealing with rotating blades, (Ref. 22). Indeed, the dynamic loading acting on a rotating blade is generally difficult to measure, and therefore the modal parameter identification procedure based on the mobility measurements cannot be successfully applied. Finally, the developed "Output-Only" procedure will be applied for the identification of the dynamic behaviour of the rotating blade. The effects of the smart hybrid active rotor control on both the modal parameters and on the response of the whole Mach-scaled rotating blade model will be investigated by considering only the measurements of the time responses.

Subsystem Flap. In SHARCS, trailing edge flap actuator will be a Carleton-modified version of the "X-frame" actuator (Ref. 26), shown in Fig. 15. Hall, et al. at the Massachusetts Institute of Technology invented this actuator for the same application (to actuate a trailing edge flap in a Mach-scaled rotor). Due to the fact that all members in an "X-frame" actuator are active, that is, none are simply serving as a "dead bar" or support, and all members are loaded, the "X-frame" is a high specific work device. The improved "X-frame" concept is currently

undergoing detailed design and analysis at Carleton University.

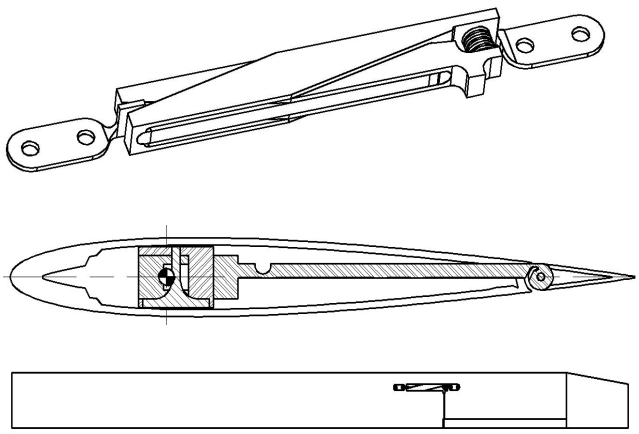

Fig. 15: SHARCS "X-frame" flap actuator (top); installed in the blade cross section (middle) and along the blade (bottom).

Subsystem Anhedral Angle Control. Shape memory alloy wires will actuate the system designed at Carleton University. These wires will run longitudinally along the blade for a distance sufficient to develop useful strains to perform the required actuation. A 20 degree deflection in the tip anhedral angle is expected. The aeroelastic similarity in the tip anhedral itself was discarded due to its relative size and stiffness. A position control feedback system is currently under development at Carleton University to maintain the anhedral angle at a given set under perturbations in loading and temperature (Fig. 16).

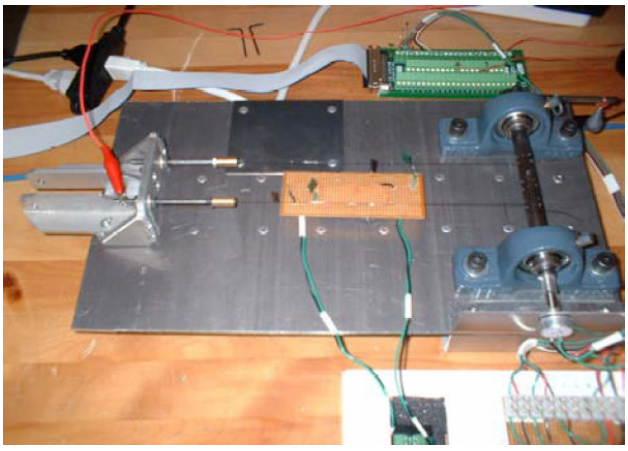

Fig. 16: Anhedral Control System using Shape Memory Alloy wires.

A series of wind tunnel tests is planned at Carleton University to evaluate the change in vortex shedding patterns as a function of a number of variables, including, but not limited to, the angle of the hinge line with respect to the spanwise direction, the inclusion of inboard winglets to manage forces, and the effect of the line where the "fold" occurs. The models will be made at Carleton University rapid prototyping machine.

Complete System Simulations

To further support the experimental activities, a multi-body modeling and simulation of the complete system including the structural and flow control systems is under the responsibility of POLIMI (Fig. 17). The multi-body general approach to the analysis of the dynamics of deformable, actively controlled systems allow the time-integration of the equations of motion of arbitrarily complex dynamic systems such as proposed in SHARCS (Ref. 27).

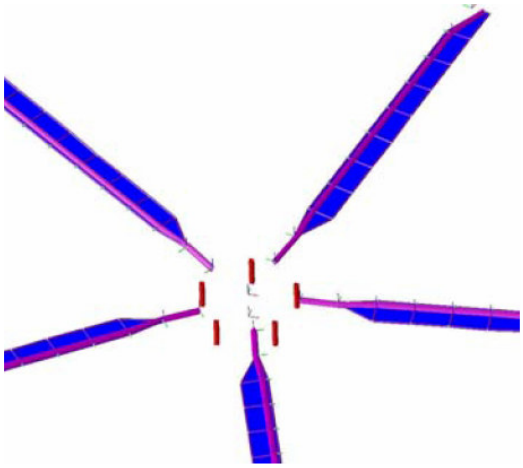

Fig. 17: SHARCS project rotor system modeled by POLIMI.

In the case of the semi-active pitch link, accurate simulations of the dynamics of the system can be performed without resorting to unnecessary simplifications. The rotor is modeled by considering the exact kinematics of the rigid components, including those of the conventional swash-plate. Geometrically exact nonlinear beam elements and increasingly refined aerodynamic models that include the free wake effect will be used to model the rotor blades. The dynamics problem will be then written in form of differential algebraic equations of order three, and integrated with A/L-stable multi-step algorithms. The differential part of the problem is represented by the dynamics of the system, written as a collection of free bodies connected by deformable elements in the form:

$$\begin{cases} M(u)\,\dot{u} = p \\ \dot{p} = F(u,\dot{u}) \end{cases} \tag{6}$$

In (6), M is the inertia matrix, and u, p and F are the arrays collecting the kinematical physical degrees-of-freedom, moments and configuration-dependent forces, respectively.

A finite-volume approach is used to formulate the forces and moments exchanged between the rigid bodies as functions of their relative positions and orientations. An intrinsic formulation in terms of strain and curvature and their time derivatives allow the introduction of consistent deformable elements, proved suitable for the description of the dynamics of the rotor blades (Refs. 27, 28). The kinematic constraints are described by algebraic equations, and result in the addition of the internal forces as Lagrange multipliers, λ:

$$\begin{cases} M(u)\,\dot{u} = p \\ \dot{p} + \Phi_{/u}^{T}\lambda = F(u,\ \dot{u}) \\ \Phi(u) = 0 \end{cases} \tag{7}$$

This approach also allows modeling of the semi-active pitch link in detail, including the friction forces resulting from the sliding and the striction present in the axial impedance control device. In general, friction effects are accounted for using a combination of friction models and shape functions. The friction model is independent from the contact geometry and computes, given the normal force and the relative velocity between the parts, the friction coefficient of an ideal, conform contact (Ref. 29). The shape function, on the other end, accounts for the real geometry of the contact, and allows computing, knowing the friction coefficient and the normal reaction force, the global of friction effect in terms of force and/or moment components. The friction model should at least be able to reproduce the striction and the dependency of the friction coefficient on the relative sliding velocity, e.g. the Stribeck effect.

All friction laws can be combined using shape functions. Currently, the multi-body code at POLIMI, MBDyn, provides two different friction models. The first is a classic Coulomb friction model that imposes striction with an algebraic constraint on the relative displacement of the contacting parts. This friction model proved to be very efficient but it does not account for friction memory effects and elastic pre-sliding. Therefore, a second friction model – a modified LuGre friction model (Ref. 30), considers an internal state instead of discrete state transitions to deal with the problem of striction. The resulting friction model can reproduce striction, elastic relative displacements before sliding, the Stribeck effect and, importantly, the memory effect that has been observed in sliding contacts with velocity variations. This model will be linearized analytically, thus allowing for a fast and robust implicit time integration of the equations of motion.

Wind Tunnel Tests

The two rotating blade wind tunnel tests will take place at POLIMI not before the summer of 2007. In a first test, the system identification will be performed. In a subsequent test, the efficiency of the hybrid control system to control noise and vibration simultaneously will be evaluated. The collaborators will jointly participate in the data acquisition process and in the data reduction to produce the SHARCS final report.

Acknowledgements

The authors would like to thank of the support of Dr. E. Bianchi (project coordinator), Eng. V. Caramaschi and Eng. G. Crosta from Agusta S.p.A. of Italy for important discussions. Also the contribution of their graduate students from Carleton University directly involved with some of the material presented in this paper is greatly appreciated: D. Brassard, G. Oxley, G. Davis and T. Mikjaniec.

References:

1. Splettstoesser, W. R. et. al., “The HELINOISE Aeroacoustic Rotor Test in the DNW – Test Documentation and Representative Results”, DLR-Mitt. 93-09, DLR, Braunschweig, Germany, 1993.

2. Nitzsche, F., Grewal, A. and Zimcik, D. G., 1999, Structural Component having Means for Actively Varying its Stiffness to Control Vibrations, U.S. Patent No. 5,973,440. European Patent: EP-996570-B1, 2001.

3. Nitzsche, F., Zimcik, D., Wickramasinghe, V. and Yong, C., “Control Laws for an Active Tunable Vibration Absorber Designed for Aeroelastic Damping Augmentation,” The Aeronautical Journal, Vol. 108, No. 1079, 2004, pp. 35-42.

4. Feszty, D., Gillies, E. A., Vezza, M., “Alleviation of Airfoil Dynamic Stall Moments via Trailing Edge Flap Flow Control”, AIAA Journal, Vol. 42, no.1, pp 17-25, January 2004.

5. Aoyama, T. et al., "Calculation of Rotor Blade-Vortex Interaction Noise using Parallel Super Computer," Paper 81, Proceedings: 22nd European Rotorcraft Forum, The Royal Aeronautical Society, Vol. 2, 1996.

6. Hodges, D. H., and Dowell, E. H., "Nonlinear Equation for the Elastic Bending and Torsion of Twisted Non-uniform Rotor Blades," NASA TN D-7818, 1974.

7. Hodges, D. H. and Ormiston R. A., "Stability of Elastic Bending and Torsion of Uniform Cantilever Rotor Blades in Hover with Variable Structural Coupling," NASA TN D-8192, 1976.

8. Theodorsen, T., "General Theory of Aerodynamic Instability and the Mechanism of Flutter", NACA Report 496, 1935.

9. Greenberg, J. M., "Airfoil in Sinusoidal Motion in a Pulsating Stream," NACA TN-1326, 1947.

10. Drees, J. M., "A Theory of Airflow Through Rotors and Its Application to Some Helicopter Problems," Journal of the Helicopter Association of Great Britain, Vol. 3, No. 2, pp. 79-104, 1949.

11. Gennaretti, M., and Carvai, A., "Aeroelastic Modeling and Vibratory Load Analysis of Helicopters," International Conference on Computational and Experimental Engineering and Science, Madeira, Portugal, July 2004.

12. Knollseisen, M., "Studio di un Sistema Semi-Attivo per la Riduzione delle Vibrazioni al Mozzo di Elicotteri in Volo d'Avanzamento," Tesi di Laurea, University of Rome 'Roma Tre', 2005 (in Italian).

13. Zhang, J., "Active-Passive Hybrid Optimization of Rotor Blades with Trailing Edge Flaps," Ph.D. Thesis, Department of Aerospace Engineering, The Pennsylvania State University, 2001.

14. Gandhi, F., and Anusonti-Intra, P., "Helicopter Vibration Reduction using Discrete Controllable-Stiffness Devices at the Rotor Hub," AIAA Paper 2001-1438, Proceedings of the 42nd AIAA/ASME/ASCE/AHS/ASC Structures, Structural Dynamics, and Material Conference, Seattle, Washington, 2001.

15. Opoku, D. and Nitzsche, F., "Acoustic Validation of a New Code Using Particle Wake Aerodynamics and Geometrically Exact Beam Structural Dynamics," Paper No. 11, Proceedings: 29th European Rotorcraft Forum, 16-18 September 2003, Friedrichshafen, Germany.

16. Nitzsche, F., Harold, T., Wickramasinghe, V. K., Young, C. and Zimcik, D. G., "Development of a Maximum Energy Extraction Control for the Smart Spring," Journal of Intelligent Material Systems and Structures (accepted for publication, 2005).

17. Rossini, L., "Controlli Semi-Attivi Basati su Flap al Bordo di Uscita per la Riduzione dei Carichi Aeroelatici Vibratori al Mozzo di un Elicottero,'" Tesi di Laurea, University of Rome 'La Sapienza', 2005 (in Italian).

18. "NTUA Internal Report on the GAST code", Aerodynamics Laboratory, Department of Mechanical Engineering, National Technical University of Athens, Greece, 2005.

19. Badcock, K.J., Richards, B.E. and Woodgate, M.A. "Elements of Computational Fluid Dynamics on Block Structured Grids Using Implicit Solvers", Progress in Aerospace Sciences, vol 36, pp 351-392, 2000.

20. Davis, G.L., Feszty, D., Nitzsche, F., "Trailing Edge Flap Flow Control for the Mitigation of Dynamic Stall Effects", paper no. 053, 31st European Rotorcraft Forum, Florence, Italy, 12-14 September 2005.

21. Wierach P., Personal Communication, Carleton University, 2004.

22. Balis Crema, L., Coppotelli, G., "Output-Only Approach for Finite Element Model Updating of AB-204 Helicopter Blade", in Proceedings of 46th AIAA/SDM Conference, 18-22/Apr./2005, Austin, TX, USA, paper No. AIAA-2005-2249.

23. Brincker, Zhang, R. L., and Andersen, P. "Modal Identification from Ambient Responses Using Frequency Domain Decomposition", XVIII IMAC, 07-10/Feb., San Antonio (TX) - USA, 2000.

24. Brincker, R., Ventura, C. E. and Andersen, P., "Why Output-Only Modal Testing is a Desirable Tool for a Wide Range of Practical Applications, " XXI IMAC, 3-6/Feb., Orlando (FL) - USA, (2003), pp. 265-272.

25. Agneni, A., Brincker, R., Coppotelli, G., "On Modal Parameters Estimates from Ambient Vibration Tests," in Proceedings of International Seminar on Modal Analysis, Leuven, Belgium, 2004.

26. Hall, S. R., Tzianetopoulou, T., “Design and testing of a double X-frame piezoelectric actuator,” Smart Structures and Materials 2000: Smart Structures and Integrated Systems, Vol. 3985, 2000.

27. Ghiringhelli, G. L., Masarati, P., and Mantegazza, P., “Analysis of an Actively Twisted Rotor by Multibody Global Modelling,” Composite Structures, April 2001, Vol. 52/1, pp. 113-122.

28. Ghiringhelli, G. L., Masarati, P., and Mantegazza, P., “A Multibody Implementation of Finite Volume Beams,” AIAA Journal, Vol. 38(1), January 2000, pp. 131-138.

29. Armstrong-H´elouvry, B., Dupont, P., and Canudas de Wit, C., “A survey of models, analysis tools and compensation methods for the control of machines with friction,” Automatica, 30(7): 1083–1138, 1994.

30. Dupont, P., Hayward, V., Armstrong, B., and Altpeter, F., “Single state elastoplastic friction models,” IEEE Transactions on Automatic Control, 47(5):787–792, May 2002